THE DYNAMICAL STRESS DISTRIBUTIONS OF STIFFENED PLATE CONTAINING WEB FRAMES DURING VIBRATION

SHIMIZU, Shigetoshi
Research Institute for Applied Mechanics, Kyushu University : Associate Professor

SATO, Masashi
Kitakyushu Technical College : Associate Professor

https://doi.org/10.5109/7172178

出版情報：Reports of Research Institute for Applied Mechanics. 19 (63), pp.101-124, 1971. 九州大学応用力学研究所

Reports of Research Institute for Applied Mechanics
Vol. XIX, No. 63, 1971

THE DYNAMICAL STRESS DISTRIBUTIONS OF STIFFENED PLATE CONTAINING WEB FRAMES DURING VIBRATION

By Shigetoshi SHIMIZU* and Masashi SATO**

The eigen-values and the dynamical stress distributions of the stiffened plate containing web frames are analyzed theoretically. As a numerical example, the free vibration of forepeak tank bulkhead of 67,800 T. D. W. tanker, the web and ordinary frames are arranged alternately, is treated.

The effect of the aspect ratio of panel on the lowest eigen-value and the corresponding mode are very important.

The effects of the bending stiffness of the ordinary frame on the mode shape are hardly recognized for the large values of aspect ratio of panel, but it becomes important factors for the small values of aspect ratio.

An approximate calculation method of the eigen-values of the stiffened plate contained web frames is introduced, the calculation results agree fair well with the exact solutions.

The considerably high dynamical bending stress concentrates at each joint of the plate and stiffeners.

1. Introduction

Author's report[1] treated in details the dynamical bending stress distributions and the plane stress of vibrating stiffened plate, and analysed the causes of the crack damage of the joints of plate and stiffeners of ship structures.

Using the previous method[1], in this report, we analyse the dynamical stress distributions of the stiffened bulkhead at the engine room or the forepeak tank of the middle class tanker such as 70,000 T. D. W., on whose bulkhead plate the web frames are arranged between the ordinary frame and the other reciprocally.

Also, we introduce the approximate formulas for the four typical normal modes of the semi-infinite long stiffened plate, whose dimenions and the arrangement of the stiffeners are same as an anactual bulkhead. Comparing these approximate formulas with the exact solutions, we can conclude they give so good approximate eigen-values and stress distributions.

* Associate Professor, Research Institute for Applied Mechanics, Kyushu University.
** Associate Professor, Kitakyushu Technical College.

2. Assumptions

We make the same assumptions as the previous report[1], that is:

1) The plate is stiffened in one direction, and simply supported along two edges which are perpendicular to the stiffeners.

2) Though all the ends of the stiffeners are restrained for torsional rotation, they are free to warp.

3) Since the natural frequencies of the longitudial vibration of stiffeners are extremely higher than those of the lateral vibration, the effect of the longitudinal vibration of the stiffeners is neglected.

4) The cross-sectional distortion of stiffeners is neglected.

5) * The tangential component of inertia forces of the plate is so small compared with the normal ones that it is neglected. The plane-stress condition of the plate can be assumed as the statical two dimensional problems.

Notation

x, y, z : Rectangular co-ordinates (Fig. A 1.1)
L : Length of plate or stiffener
B : Frame space
E : Young's modulus of elasticity
ν : Poisson's ratio
t_p : Thickness of plate
t_s : Thickness of web plate of stiffener

$D=\dfrac{Et_p{}^3}{12(1-\nu^2)}$ Flexural rigidity of plate

$\theta = \bar{\theta}\, sin\dfrac{n\pi}{L}x\; e^{i\omega t}$ Rotation around x axis

$$\left.\begin{aligned} u &= \bar{u}\, cos\frac{n\pi}{L}x\; e^{i\omega t} \\ v &= \bar{v}\, sin\frac{n\pi}{L}x\; e^{i\omega t} \\ w &= \bar{w}\, sin\frac{n\pi}{L}x\; e^{i\omega t} \end{aligned}\right\}\ \text{Displacements in direction of } x,\ y \text{ and } z \text{ axis}$$

$\lambda = \dfrac{n\pi B}{L}$

$\kappa = \left(\dfrac{\gamma t_p \omega^2}{gD}\right)^{\frac{1}{4}}\cdot B$ Eigen-value

ω : Circular frequency
γ : Weight of material of plate or stiffener per unit volume

* C. S. Smith[2] analysed the vibration of stiffened plate included the dynamical terms in plane-stress.

$\mu = \frac{1+\nu}{2\lambda}$

a, b, c, d, e, g : Functions of λ

a', b', c', d', e', g', : Functions of λ and κ

M_y : Bending moment per unit length of section of plate perpendicular to y axis

V_y : Force per unit length of section of plate perpendicular to y axis

$$\left.\begin{aligned} q_{Ax} &= \bar{q}_{Ax} \cos\frac{n\pi}{L}x \; e^{i\omega t} \\ q_{Ay} &= \bar{q}_{Ay} \sin\frac{n\pi}{L}x \; e^{i\omega t} \\ q_{Az} &= \bar{q}_{Az} \sin\frac{n\pi}{L}x \; e^{i\omega t} \end{aligned}\right\}$$

Forces per unit length of the intersection of stiffener and plate in direction of x, y and z axis

$m_{Ax} = \bar{m}_{Ax} \sin\frac{n\pi}{L}x \; e^{i\omega t}$ Moment per unit length of the intersection of stiffener and plate parallel to x axis

A_s : Sectional area of stiffener

m_{st} : Mass per unit length of stiffener

$\{\bar{P}_p\} = \{\bar{s}_{jk} \; \bar{s}_{kj} \; \bar{p}_{jk} \; \bar{p}_{kj}\}$

$\{\bar{U}_p\} = \{\bar{u}_j \; \bar{u}_k \; \bar{v}_j \; \bar{v}_k\}$

$\{\bar{P}_b\} = \{\bar{V}_{yjk} \; \bar{V}_{ykj} \; \bar{M}_{yjk} \; \bar{M}_{ykj}\}$

$\{\bar{U}_b\} = \{\bar{w}_j \; \bar{w}_k \; \bar{\theta}_j \; \bar{\theta}_k\}$

Subscripts and Superscript :

j, k : j and k side of plate

A : Intersection of stiffener and plate

p : State of plane stress of plate

b : Bendig of plate

3. General Expression of the Characteristic Equation to the Stiffened Plate

The dynamical equilibrium equation at the mth intersection of plate and stiffener is shown in Appendix 4 as follows,

$$\boldsymbol{K}_1 \boldsymbol{U}_{m-1} + \boldsymbol{K}_D \boldsymbol{U}_m + \boldsymbol{K}_2 \boldsymbol{U}_{m+1} = \boldsymbol{0} \tag{3.1}$$

The elements B_{ij} and D_{ij} of the matrix K_D characterize the static and dynamic effect of the stiffener as shown Appendix 3. Therefore if we use the suffix W for the web frame, reference to Eq. (3.1), we obtain the equilibrium equations at the mth intersection of plate and web frame as follows,

$$\boldsymbol{K}_1 \boldsymbol{U}_{m-1} + \boldsymbol{K}_{DW} \boldsymbol{U}_m + \boldsymbol{K}_2 \boldsymbol{U}_{m+1} = \boldsymbol{0} \tag{3.2}$$

In the same way, the equilibrium equation at the nth intersection of plate and ordinary frame is expressed as,

$$\boldsymbol{K}_1 \boldsymbol{U}_{n-1} + \boldsymbol{K}_{DO} \boldsymbol{U}_n + \boldsymbol{K}_2 \boldsymbol{U}_{n+1} = \boldsymbol{0} \tag{3.3}$$

where the suffix O denotes an ordinary frame.

Especially if an ordinary frame is arranged between two web frames alternately with the same space on the stiffened plate, the equilibrium equations are introduced using the equations (3.2) and (3.3) as,

$$\begin{bmatrix} \boldsymbol{K}_{DO} & \boldsymbol{K}_2 & & \\ \boldsymbol{K}_1 & \boldsymbol{K}_{DW} & \boldsymbol{K}_2 & \\ & & \ddots & \\ & & \boldsymbol{K}_1 & \boldsymbol{K}_{DO} \end{bmatrix} \begin{bmatrix} \boldsymbol{U}_1 \\ \boldsymbol{U}_2 \\ \vdots \\ \boldsymbol{U}_n \end{bmatrix} = \begin{bmatrix} \boldsymbol{0} \\ \boldsymbol{0} \\ \vdots \\ \boldsymbol{0} \end{bmatrix} \tag{3.4}$$

The set of equations described by (3.4) is a set of algebraic, linear, homogeneous equations. By Cramer's rule, it follows that there can be other than trivial values of the $\boldsymbol{U}_m$ only if the determinant of the coefficients of $\boldsymbol{U}_m$ vanishes. This implies the necessity of

$$\begin{vmatrix} K_{DO} & K_2 & & \\ K_1 & K_{DW} & K_2 & \\ & & \ddots & \\ & & K_1 & K_{DO} \end{vmatrix} = 0 \tag{3.5}$$

where K_1, K_2, K_{DO}, K_{DW} represent the elements of the matrix $\boldsymbol{K}_1$, $\boldsymbol{K}_2$, $\boldsymbol{K}_{DO}$, $\boldsymbol{K}_{DW}$, respectively.

By assuming a deflection, for example, the lateral deflection of the rth intersection w_r is equal to unit, we can solve the equation (3.4) for each eigen-value obtained from the characteristic equation (3.5).

By substituting the eigen-vectors $\boldsymbol{U}$ obtained from the Eq. (3.4) into following equtions (reference Appendix 1 and 2), we can calculate the dynamical stress components of the midsurface of the plate, the tranverse bending moment and deflection.

$$My = -(D/B)[[\psi''] - \nu\lambda^2[\psi]]\{\boldsymbol{U}_b\} \sin n\pi\xi e^{i\omega t} \tag{3.6}$$

$$w = B[\psi]\{\boldsymbol{U}_b\} \sin n\pi\xi e^{i\omega t} \tag{3.7}$$

$$\sigma_x = [\phi''][k_p]\{\boldsymbol{U}_p\} E \sin n\pi\xi e^{i\omega t} \tag{3.8}$$

4. Calculation Results

Fig. 4.1 shows a part of the forepeak tank bulkhead of 67,800 T.D.W. tanker. Let us consider this bulkhead simply as a rectangular stiffened plate simply supported along its two edges which are perpendicular to the stiffeners, while clamped along the others as shown in Fig. 4.2. We treat two kinds of stiffeners in our calculation; one is called the ordinary frames which is a flat bar (125×12), and the other is called the web frame which is a inverted angle (200×90×9/14). We arrange 6 ordinary frames and 5 web frames in the same space $B = 455$ mm from each other. Each stiffener is 4,600 mm long, and whose length is the mean value of the distance between the upper

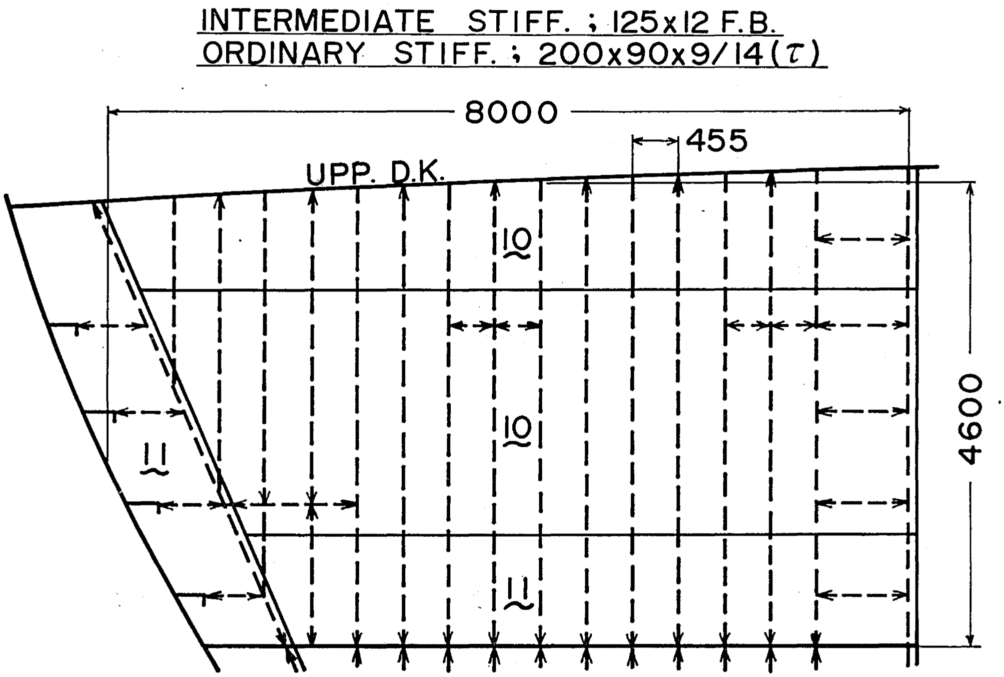
INTERMEDIATE STIFF. ; 125x12 F.B.
ORDINARY STIFF. ; 200x90x9/14(τ)
8000
455
UPP. D.K.
10
10
11
11
4600

Fig. 4.1

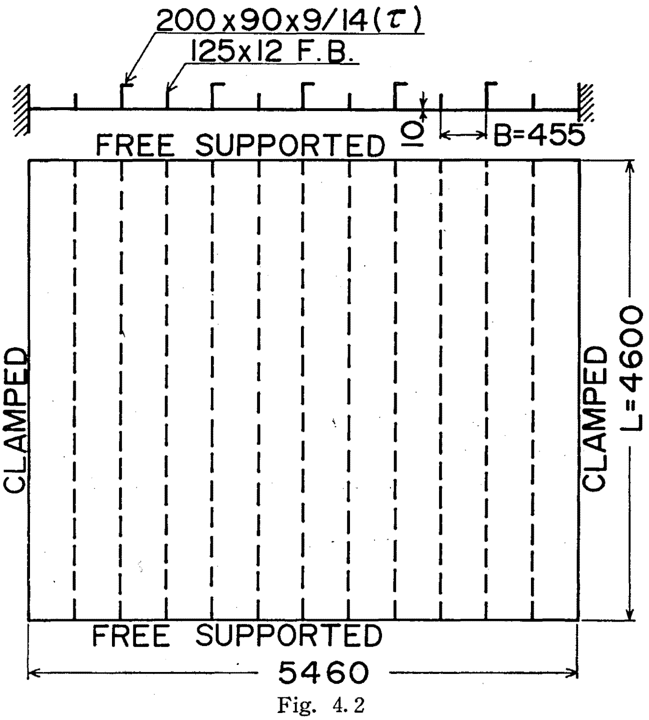
200x90x9/14(τ)
125x12 F.B.
10
B=455
FREE SUPPORTED
CLAMPED
CLAMPED
L=4600
FREE SUPPORTED
5460

Fig. 4.2

deck and the horizontal girder. The thickness of the plate is assumed uniformly 10 mm. In this case $\lambda=\pi B/L=0.311$, we investigate the effect of the aspect ratio of the panel on the eigen-values, mode shapes and dynamical stress distributions, changing the values of λ as follows; $\lambda=0.2,\ 0.4,\ 0.6,\ 1.0,\ 1.5,\ 2.2$.

Fig. 4.3 shows the typical modes and stress distributions during vibration

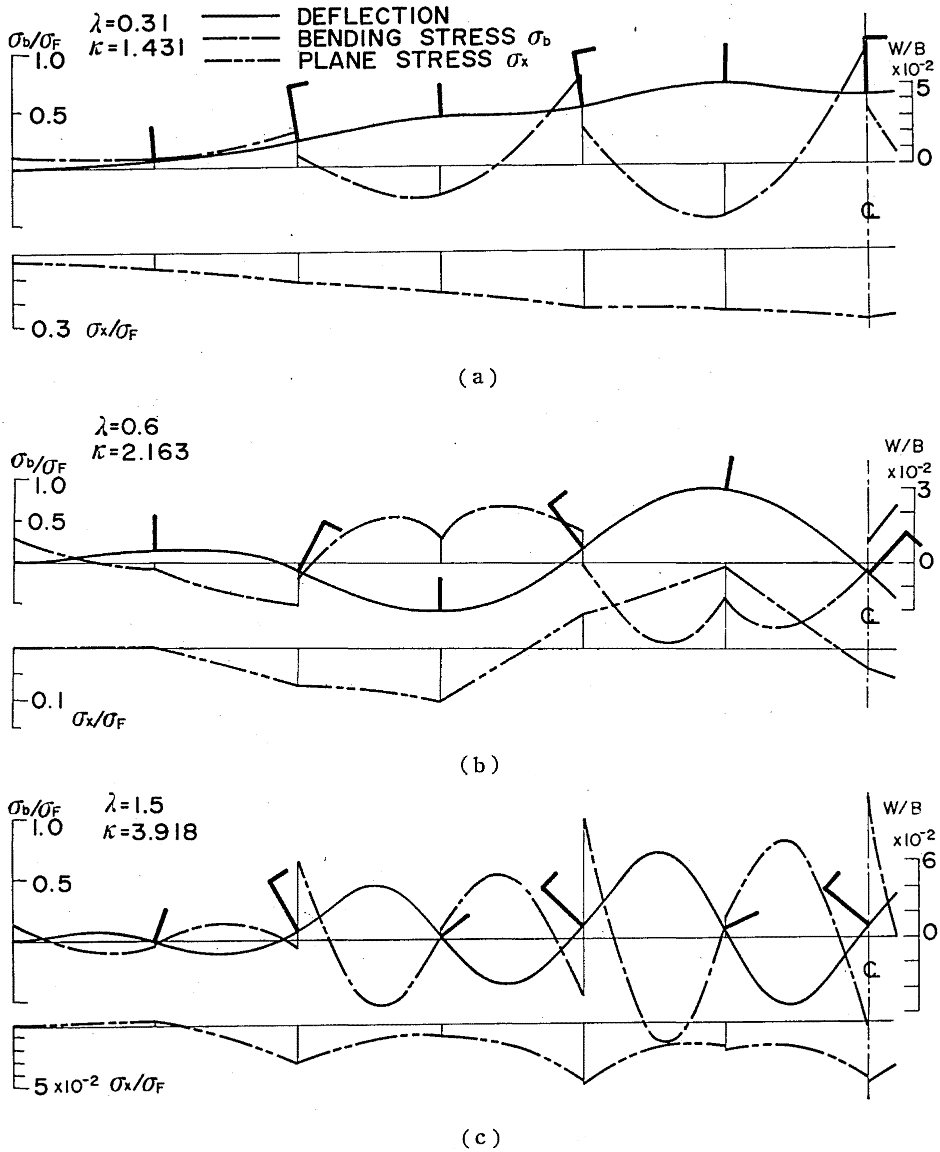

Fig. 4.3

for three different λs: 0.31, 0.6 and 1.5. Since the mode shape of each λ is almost symmetry about the centre line of the stiffened plate, we show the mode shapes of the left side of it.

The bending stress curves in Fig. 4.3 are plotted by the ratio of the bending stress σ_b and the fatigue limit of the material of the stiffened plate, on the assumption that the maximum bending stress is equal to the fatigue limit $\sigma_F = 22\,\mathrm{kg/mm^2}$. We plot also the inplane stress σ_x which is expressed

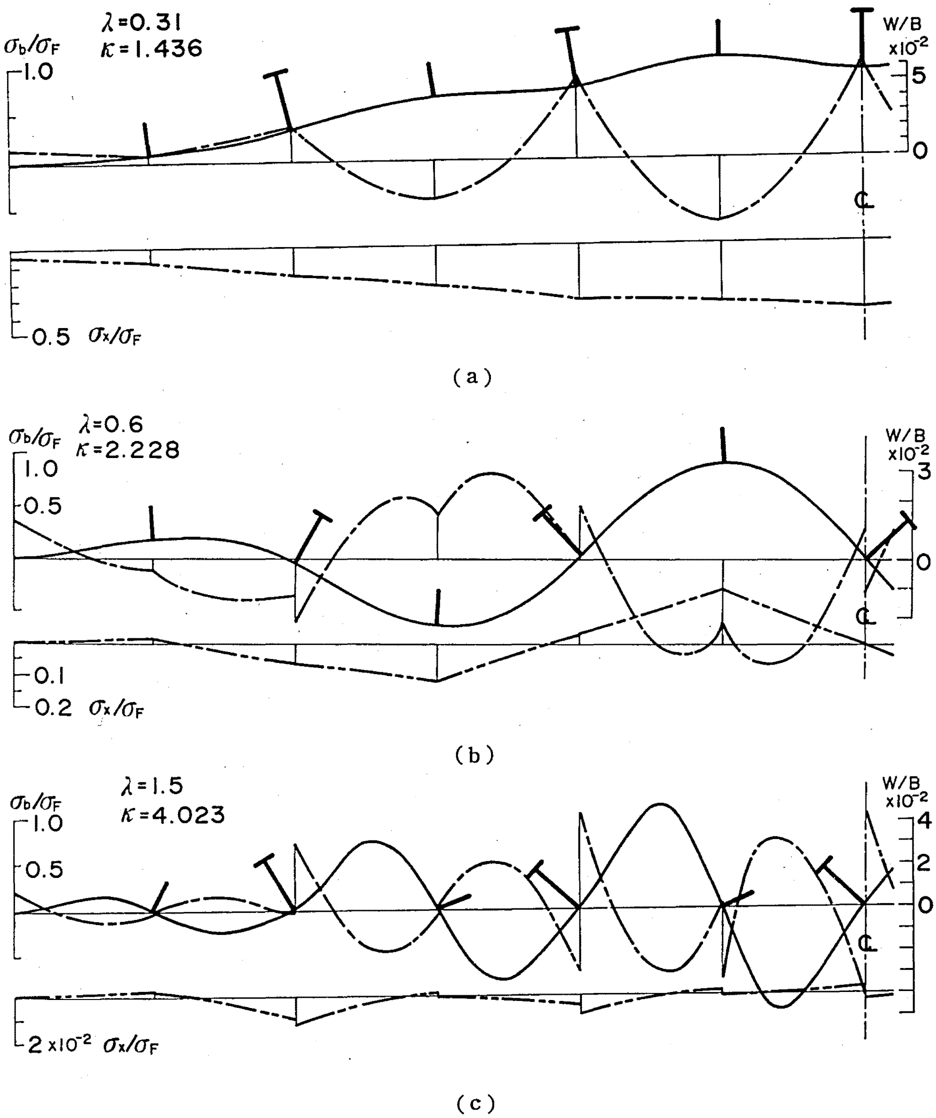

Fig. 4.4

same manner as the bending stress.

Assuming the fatigue limit is equal to 22 kg/mm^2, we find the ratio of the maximum deflection of the stiffened plate and the frame space B, corresponding to the maximum bending stress in the plate gets to their fatigue limit. We show the calculated values of $(w/B)_{max}$ in Table 1 with the natural frequencies cycle per minute.

Table 1 The ratio of the maximum deflection w_{max} and the frame space B, when the maximum bending stress on the plate gets to the fatigue limit $\sigma_F=22$ kg/mm^2. (The dimensions of the stiffened plate are shown in Fig. 4.2.)

λ	L/B	CASE	$(w/B)_{max}$	frequency (cpm)
0.311	10.1	1	4.95×10^{-2}	1,470
0.6	5.2	2	2.95×10^{-2}	3,370
1.5	2.1	3	0.616×10^{-2}	11,050

In Fig. 4.3 (a) corresponding to the stiffened plate shown in Fig. 4.2, the aspect ratio of the panel L/B is equal to 10.1, since the ratio is fairly large, the apparent bending rigidity EI/L of the web and ordinary frame are small. Therefore, each stiffener deflects in the same direction and the stiffened plate vibrates transversely as a whole.

From the bending stress distribution, we find out that the plate between the two web frames is almost clamped at the intersection of the plate and web frames, while the deflection of ordinary frames are pretty large and their inertia forces act on the plate as the concentrated force. Therefore, we see the pretty high stress concentration at the intersections of the plate and web or ordinary frames. Since the distribution of the inplane stress σ_x is nearly uniform, the effective breadth of the plate is approximately equal to the stiffener space.

When the aspect ratio is comparatively small value, say $L/B=5.3$ ($\lambda=0.6$), the ordinary frames still vibrate transversely, but the web frame vibrate torsionally as shown in Fig. 4.3 (b). Since the length of the stiffeners are small, the apparent bending rigidity of the ordinary frame becomes higher than the rigidity of the case of $\lambda=0.31$, and therefore the effect of the ordinary frame on the bending stress distribution is large in the bending rigidity rather than the inertia force as we see the bending stress distribution in Fig. 4.3 (b).

When the aspect ratio of the panel becomes smaller, say $L/B=2.1$ ($\lambda=1.5$), we see both of the ordinary and web frame vibrate torsionally, as shown in Fig. 4.3 (c), but the distribution of bending stress shows the edges of the plate at the intersection of the web frames are almost clamped, and then it may be considered that the direction of the rotatory vibration of web frames reduce the slope of the plate at their intersections.

In order to simplify the calculation, the web frame constructed by the inverted angle shown in Fig. 4.2 is replaced by the symmetrical T-section of the same dimensions of the inverted angle. We calculate about the same aspect ratio as previous example, and the results are shown in Fig. 4.4 (a), (b) and (c) for $\lambda = 0.31$, 0.6 and 1.5, respectively.

Fig. 4.4, as compared with Fig. 4.3, show almost the same result in the mode curves and the distributions of inplane and bending stress. But we must take care of the fact that the eigen-values for the stiffened plate with the symmerical stiffeners are 2 or 3 % higer than those for the stiffened plate which has the same dimensions but with the stiffeners of unsymmetrical section.

5. Approximate Calculation Methods

Under the assumptions in the Section 2, we can analyse the vibration of any stiffened plate with the given dimensions, arrangement and number of web and ordinary frames, and on the given boundary conditions at the edges of the plate. If the stiffened plate has the great number of stiffeners, in addition to, it is regularly arranged by the web and ordinary frames, on the assumption that this stiffened plate is the semi-infinite long stiffened plate which has the same dimensions of plate and stiffener, we can calculate the approximate eigen-values by assuming the typical vibrating modes.

As an example, we illustrate the approximate method to the stiffened plate arranged with an ordinary frame between two web frames alternately as described in previous section. We assume four cases of modes of vibration as shown in Fig. 5.1 (a), (b), (c) and (d). In case 1, the deflections of each web and ordinary frame are the same, respectively, and the transverse slopes of each stiffener are equal to zero. In case 2, the deflections of the ordinary frames have the same values in magnitude but opposite in direction, and transverse slopes are equal to zero, on the other hand, the deflections of the web frames are equal to zero, and the transverse slope of the ordinary frame have the same values in magnitude but opposite in direction. In case 3, the deflection of the web and ordinary frames are equal to zero, each web frame rotate same direction, but opposite to the rotation of the ordinary frames. Case 4 coresponding to replace the web frames by the ordinary ones in case 2.

Substituting the boundary conditions of each case shown in Fig. 5.1 (a), (b), (c) and (d) into Eq. (3.4), we obtain the following equilibrium equations at the mth itersection for each case;

Case 1: $\bar{u}_m=\bar{u}_{m+2},\ \bar{v}_m=\bar{v}_{m+2}=0,\ \bar{w}_m=\bar{w}_{m+2},\ \bar{\theta}_m=\bar{\theta}_{m+2}=0,$
$\bar{u}_{m-1}=\bar{u}_{m+1},\ \bar{v}_{m-1}=\bar{v}_{m+1}=0,\ \bar{w}_{m-1}=\bar{w}_{m+1},\ \bar{\theta}_{m-1}=\bar{\theta}_{m+1}=0,$

$$\begin{bmatrix} 2k_{22}-B_{011} & -B_{013} & -2k_{12} & 0 \\ -B_{031} & 2k'_{22}-B_{033}-D_{033} & 0 & -2k'_{12} \\ -2k_{12} & 0 & 2k_{22}-B_{W11} & -B_{W13} \\ 0 & -2k'_{12} & -B_{W31} & 2k'_{22}-B_{W33}-D_{W33} \end{bmatrix} \begin{bmatrix} \bar{u}_{m-1} \\ \bar{w}_{m-1} \\ \bar{u}_m \\ \bar{w}_m \end{bmatrix} = \begin{bmatrix} 0 \\ 0 \\ 0 \\ 0 \end{bmatrix}$$

Case 2: $\bar{u}_m=\bar{u}_{m+2}=0,\ \bar{v}_m=\bar{v}_{m+2},\ \bar{w}_m=\bar{w}_{m+2}=0,\ \bar{\theta}_m=-\bar{\theta}_{m+2},$
$\bar{u}_{m-1}=\bar{u}_{m+1}=0,\ \bar{v}_{m-1}=-\bar{v}_{m+1},\ \bar{w}_{m-1}=-\bar{w}_{m+1},\ \bar{\theta}_{m-1}=\bar{\theta}_{m+1}=0,$

$$\begin{bmatrix} 2k_{22}-B_{011} & -B_{013} & -2k_{14} & 0 \\ -B_{031} & 2k'_{22}-B_{033}-D_{033} & 0 & -2k'_{14} \\ -2k_{14} & 0 & 2k_{44}-B_{W22}-D_{W22} & -B_{W24}-D_{W24} \\ 0 & 2k'_{14} & -B_{W42}-D_{W42} & 2k'_{44}-B_{W44}-D_{W44} \end{bmatrix} \begin{bmatrix} \bar{u}_{m-1} \\ \bar{w}_{m-1} \\ \bar{v}_m \\ \bar{\theta}_m \end{bmatrix} = \begin{bmatrix} 0 \\ 0 \\ 0 \\ 0 \end{bmatrix}$$

Case 3: $\bar{u}_m=\bar{u}_{m+2}=0,\ \bar{v}_m=\bar{v}_{m+2},\ \bar{w}_m=\bar{w}_{m+2}=0,\ \bar{\theta}_m=\bar{\theta}_{m+2},$
$\bar{u}_{m-1}=\bar{u}_{m+1}=0,\ \bar{v}_{m-1}=\bar{v}_{m+1},\ \bar{w}_{m-1}=\bar{w}_{m+1}=0,\ \bar{\theta}_{m-1}=\bar{\theta}_{m+1},$

$$\begin{bmatrix} 2k_{44}-B_{022}-D_{022} & -B_{024}-D_{024} & -2k_{34} & 0 \\ -B_{042}-D_{042} & 2k'_{44}-B_{044}-D_{044} & 0 & -2k'_{34} \\ -2k_{34} & 0 & 2k_{44}-B_{W22}-D_{W22} & -B_{W24}-D_{W24} \\ 0 & -2k'_{34} & -B_{W42}-D_{W42} & 2k'_{44}-B_{W44}-D_{W44} \end{bmatrix} \begin{bmatrix} \bar{v}_{m-1} \\ \bar{\theta}_{m-1} \\ \bar{v}_m \\ \bar{\theta}_m \end{bmatrix} = \begin{bmatrix} 0 \\ 0 \\ 0 \\ 0 \end{bmatrix}$$

Case 4: $\bar{u}_m=-\bar{u}_{m+2},\ \bar{v}_m=\bar{v}_{m+2}=0,\ \bar{w}_m=-\bar{w}_{m+2},\ \bar{\theta}_m=\bar{\theta}_{m+2}=0,$
$\bar{u}_{m-1}=\bar{u}_{m+1}=0,\ \bar{v}_{m-1}=-\bar{v}_{m+1},\ \bar{w}_{m-1}=\bar{w}_{m+1}=0,\ \bar{\theta}_{m-1}=\bar{\theta}_{m+1},$

$$\begin{bmatrix} 2k_{44}-B_{022}-D_{022} & -B_{024}-D_{024} & 2k_{14} & 0 \\ -B_{042}-D_{042} & 2k'_{44}-B_{044}-D_{044} & 0 & -2k'_{14} \\ -2k_{34} & 0 & 2k_{22}-B_{W11} & -B_{W13} \\ 0 & 2k'_{14} & -B_{W31} & 2k'_{22}-B_{W33}-D_{W33} \end{bmatrix} \begin{bmatrix} \bar{v}_{m-1} \\ \bar{\theta}_{m-1} \\ \bar{u}_m \\ \bar{u}_m \end{bmatrix} = \begin{bmatrix} 0 \\ 0 \\ 0 \\ 0 \end{bmatrix}$$

Putting the determinant of the elements of the stiffness matrix of above equations zero, we obtain the characteristic equations of vibration as shown in Table 2.

Using these equations, we calculate the eigen-values, the modes of vibration and the distributions of stress of the same stiffened plate as Fig. 4.2, for the various kinds of λ, that is, $\lambda = 0.2,\ 0.4,\ 0.6,\ 1.0,\ 2.0,\ 2.5$ and 3.0, assuming the section of the web frame is a symmetrical T-type. Fig. 5.2 shows the relation between the eigen-value κ and the aspect ratio $\lambda = \pi B/L$.

The dotted lines show the approximate eigen-values for each case, and the full line shows the lowest eigen-values for the λ s. When the values of λ are less than 0.4 ($L/B > 7.9$), the lowest eigen-values appear in case 1, and for the comparative large λ, they appear in case 2. The value of λ is larger than 2.5 ($L/B < 3.5$), we see the lowest eigen-value in case 3, and the curve for case 4 does not appear in the lowest eigen-value for any λ. When the value of λ is larger than 2.5 ($L/B < 1.3$), the curve of case 1 coincides with case 2, and the limiting value is equal to the eigen-value of the lateral vibration of the plate stiffened by an ordinary frame which is clamped at the

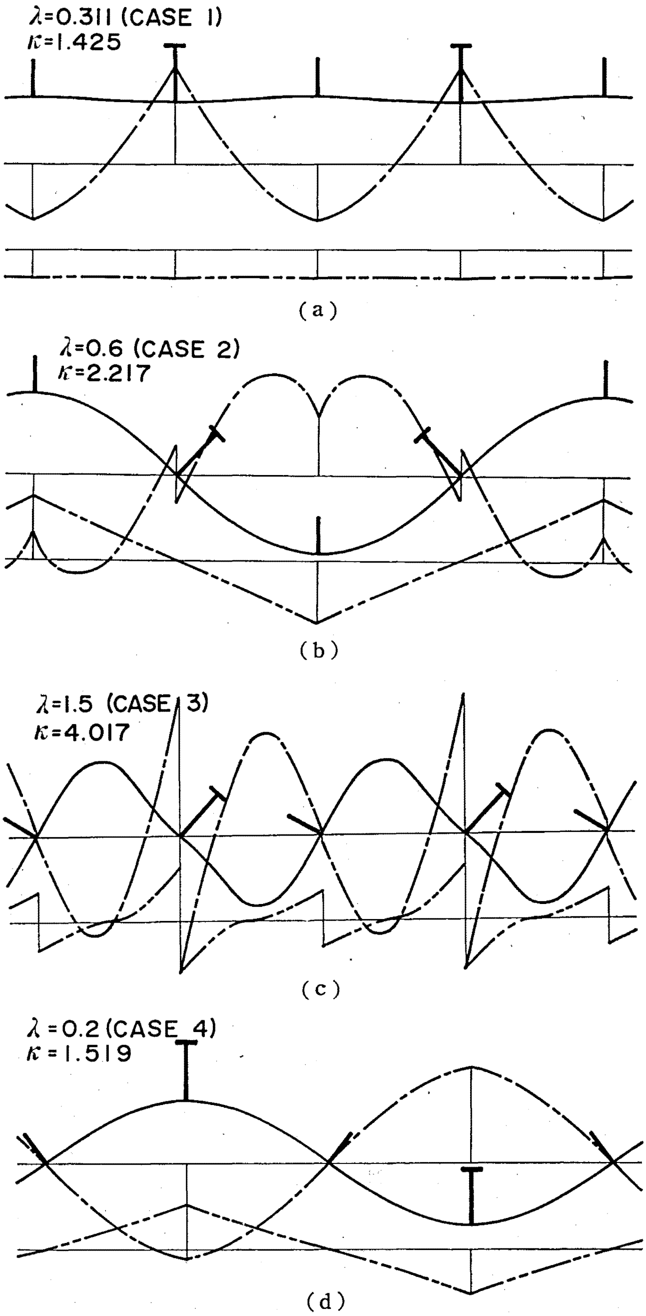

Fig. 5.1 The relation between the lowest eigen-value κ and λ for $\alpha = f^2{}_O/f^2{}_W = 0.255$

Table 2 The characteristic equations for the semi-infinite long stiffened plate

	CASE	Characteristic Equations
1	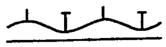	$\begin{vmatrix} 2k_{22}-B_{011} & -B_{031} & -2k_{12} & 0 \\ -B_{013} & 2k'_{22}-B_{033}-D_{033} & 0 & -2k'_{12} \\ -2k_{12} & 0 & 2k_{22}-B_{w11} & -B_{w31} \\ 0 & -2k'_{12} & -B_{w13} & 2k'_{22}-B_{w33}-D_{w33} \end{vmatrix}=0$
2	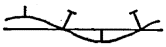	$\begin{vmatrix} 2k_{22}-B_{011} & -B_{031} & -2k_{14} & 0 \\ -B_{013} & 2k'_{22}-B_{033}-D_{033} & 0 & -2k'_{14} \\ -2k_{14} & 0 & 2k_{44}-B_{w22}-D_{w22} & -B_{w42}-D_{w24} \\ 0 & -2k'_{14} & -B_{w24}-D_{w24} & 2k'_{44}-B_{w44}-D_{w44} \end{vmatrix}=0$
3		$\begin{vmatrix} 2k_{44}-B_{022}-D_{022} & -B_{042}-D_{024} & -2k_{34} & 0 \\ -B_{042}-D_{042} & 2k'_{44}-B_{044}-D_{044} & 0 & -2k'_{34} \\ -2k_{34} & 0 & 2k_{44}-B_{w22}-D_{w22} & -B_{w24}-D_{w24} \\ 0 & -2k'_{34} & -B_{w42}-D_{w42} & 2k'_{44}-B_{w44}-D_{w44} \end{vmatrix}=0$
4	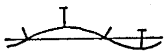	$\begin{vmatrix} 2k_{44}-B_{022}-D_{022} & -B_{024}-D_{024} & 2k_{34} & 0 \\ -B_{042}-D_{042} & 2k'_{44}-B_{044}-D_{044} & 0 & -2k'_{14} \\ -2k_{14} & 0 & 2k_{22}-B_{w11} & -B_{w13} \\ 0 & 2k'_{14} & -B_{w13} & 2k'_{22}-B_{w33}-D_{w33} \end{vmatrix}=0$

intersections of the web frames. Also the eigin-values in both case 3 and 4 approach the eigen-values for the same stiffened plate vibrating torsionally at the ordinary frame. The reason is that when the value of λ becomes large the apparent bending and torsional rigidity of the web frame increase, and the plate are nearly clamped at the intersection.

The mark ○ in Fig. 5.2 shows the exact eigen-value of the stiffened plate clamped both edges, and stiffened by 5 web and 6 ordinary frames as calculated previous section. We see the approximate eigen-values agree very well with the exact values. Comparing these results with the exact values shown in Fig. 4.3 or Fig. 4.4, we see not only the mode curves but the stress distributions agree fairly well with the exact results except the neighbour of the clamped edges.

In order to investigate the effect of the dimensions of the ordinary frame on the lowest eigen-value for the stiffened plate, using the approximate formulas in Table 2, we calculate the eigen-values of the stiffened plate which has the same dimensions as in the previous calculation, but the height of the ordinary frame changes from 0 to 200 mm which is equal to the height of the web frame. Fig. 5.3 shows the relation between the lowest eigen-value κ and α which represents the square of the ratio of the natural frequency of the transverce vibration of the ordinary frame to the natural frequency of the web frame for the various values of λs. The fat lines show the critical lines which connected the intersection points of the two curves for the different kinds of mode for the same value of λ.

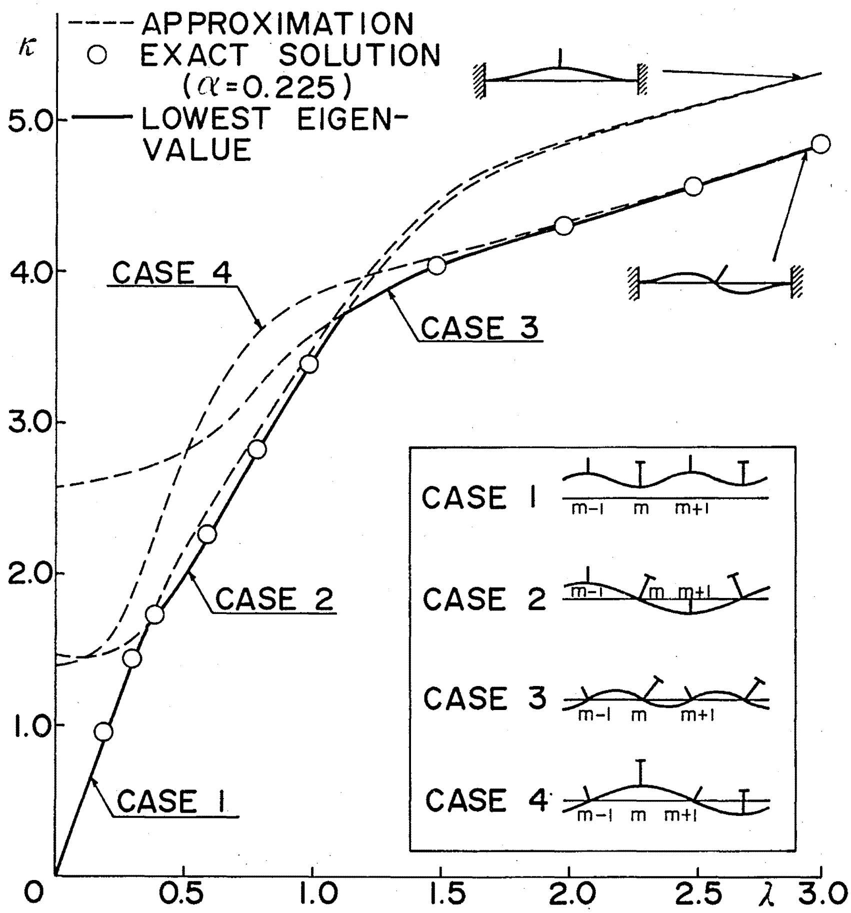

Fig. 5.2 The relation between the lowest eigen-value κ and λ for $\alpha = f^2{}_O/f^2{}_W = 0.255$

We see the mode of vibration for the lowest eigen-value changes from case 1 to case 3 with the increase of λ, but the curves for case 4 do not appear similarly to Fig. 5.2. In case 1, the mode curves for $\lambda = 0.2$ and 0.3 are almost flat, and therefore, it means that the effect of the dimensions of the ordinary frame on the lowest eigen-value of the stiffened plate is negligible so far as the maximum value of the ordinary frame is equal to the height of the web frame. But when the value of λ is comparatively large and the ordinary frames alone vibrate laterally, as case 2, the eigen-value increases with the value of α for the same λ, because the apparent bending stiffness of ordinary frame becomes large. When the value of λ is large and both the ordinary and web frame vibrate torsionally, as case 3, we see the eigen-value exibits a tendency to decrease with the increase of the height of

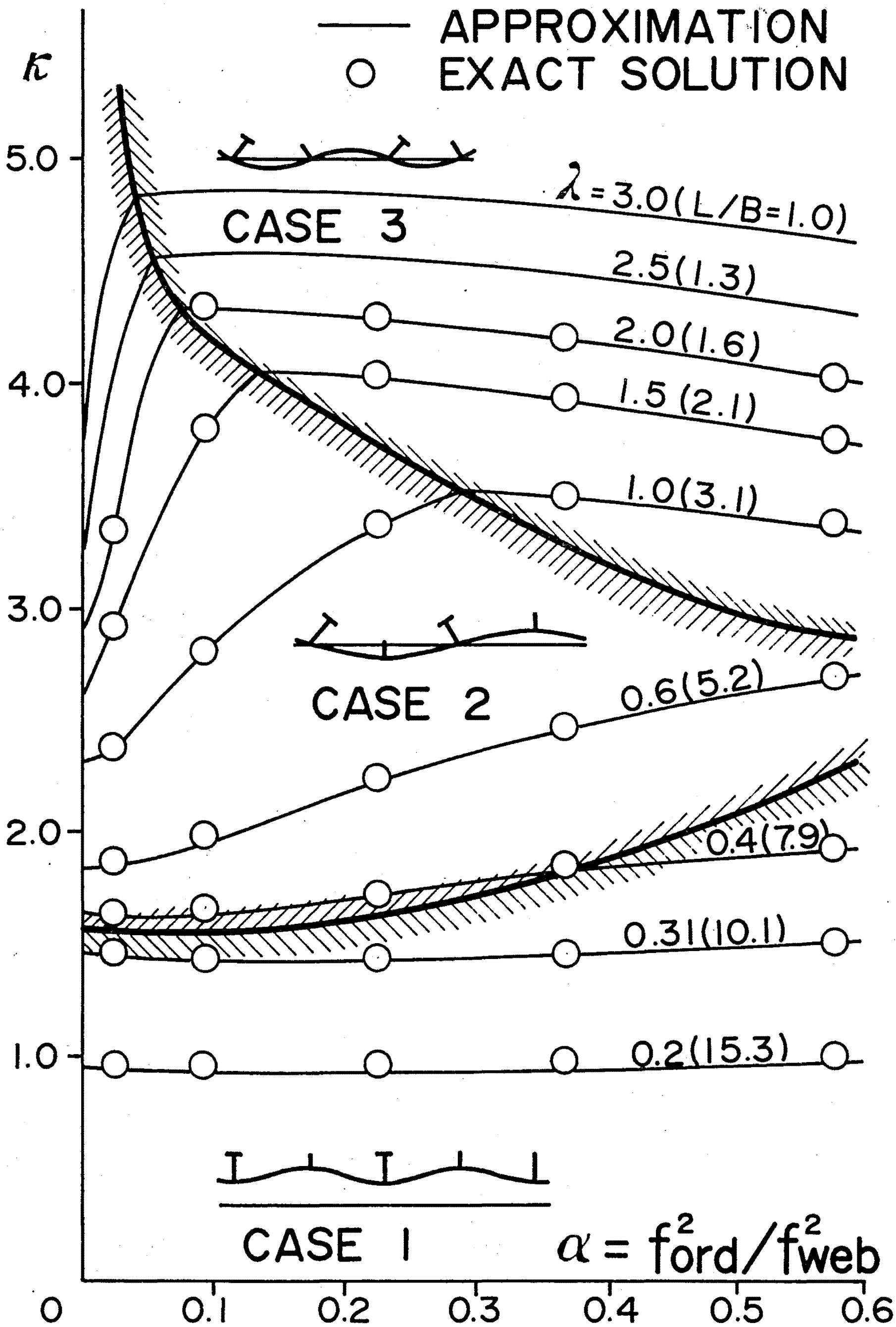

Fig. 5.3 The relation between the lowest eigen-value κ and $\alpha = f^2_O/f^2_W$ for the various values λs

the ordinary frame, and then it is due to mainly the fact that the increase of the height of the flat-bar is more effective in the increase of the weight than the torsional rigidity. The mark O in Fig. 5.3 shows the exact eigen-value of the stiffened plate clamped at both edges, and stiffened by 5 web and 6 ordinary frames, calculated by using Eq. (3.5), changing the values of λ and α. We see the approximate eigen-values agree very well with the exact values.

Since we introduced the characteristic equations in Table 2 considering the inplane stress of plate, they contain the four unknown values u, v, w and θ at a intersection of the plate and stiffener, and the characteristic equations are expressed by 4×4 determinants. If we consider the effective breadth of the plate, these unknown values become only w and θ, and we obtain the more simplified 2×2 characteristic equations as shown in Table 3. But it is complicated to calculate the effective breadth of the web and ordinary frame exactly for each mode shape. Assuming the position of the neutral axis of the section of stiffener is at the intersection of the plate and stiffener (it means the effective breadth of plate is infinite), we calculate the eigen-values by using Table 3, changing the value of λ as in the previous calculation. Table 4 shows the errors of each approximate eigen-value for the exact values of the stiffened plate as shown in Fig. 4.2. We see the maximum error is less than about 4 %.

Table 3 The approximate formulas for the eigen-values, assuming the position of the neutral axis of section of stiffener is at the intersection.

Case 1	$\begin{vmatrix} 2k'_{22}-B_{033}-D_{033} & -2k'_{12} \\ -2k'_{12} & 2k'_{22}-B_{W33}-D_{W33} \end{vmatrix}=0$
Case 2	$\begin{vmatrix} 2k'_{22}-B_{033}-D_{033} & -2k'_{14} \\ 2k'_{14} & 2k'_{44}-B_{W44}-D_{W44} \end{vmatrix}=0$
Case 3	$\begin{vmatrix} 2k'_{44}-B_{044}-D_{044} & -2k'_{34} \\ -2k'_{34} & 2k'_{44}-B_{W44}-D_{W44} \end{vmatrix}=0$
Case 4	$\begin{vmatrix} 2k'_{44}-B_{044}-D_{044} & -2k'_{14} \\ 2k'_{14} & 2k'_{22}-B_{W33}-D_{W33} \end{vmatrix}=0$

Table 4 The errors of each approximate eigen-value for the exact values of the stiffened plate as shown in Fig. 4.2.

λ	L/B	CASE	exact (Fig. 4.2)	T-section (Fig. 4.2)		approximate (Table 2)		approximate (Table 3)		Dunkerley's-formula	
			κ	κ	error %	κ	error %	κ	error %	κ	error %
0.311	10.1	1	1.431	1.436	0.3	1.425	−0.4	1.460	2.0	1.439	0.6
0.6	5.2	2	2.163	2.228	3.0	2.217	2.5	2.247	3.9	1.800	−16.8
1.5	2.1	3	3.918	4.020	2.6	4.017	2.5	4.021	2.6	2.447	−37.5

If we calculate by using the Dunkerley's formula[4],

$$1/\omega_n^2 = 1/\omega_P^2 + 1/\omega_W^2 + 1/\omega_O^2$$

where,

ω_n : circular frequency of stiffened plate

ω_P : the lowest circular frequency of the plate clamped at the joints of the stiffeners and supported freely along the other edges

ω_W : the lowest bending circular frequency of the web frame assumed the position of the neutral axis is the intersection (for case 1), or the lowest torsional circular frequency of the web frame about the axis of the intersection (for case 2 and 3)

ω_O : the lowest bending circular frequency of the ordinary frame assumed the position of the neutral axis is the intersection (case 1 and 3), or
the lowest torsional circular frequency of the ordinary frame about the axis of the intersection (for case 2).

The results calculated in terms of eigen-values are shown in Table 4. We see the approximate results for case 1 agree very well with the exact values, but for case 2 and 3, the results contain so many error that this formula is not desirable for the torsional vibration of stiffeners.

6. Conclusions

The characteristic equations and the formulas of the stress distribution of the stiffened plate contained web frames at vibration were introduced in the general form.

Especialy, the approximate calculation method of the eigen-values for the semi-infinite long stiffened plate arranged with an ordinary frame between two web frames alternately were described by assuming the vibration mode. Furthermore, we simplified this method by assuming that the position of the neutral axis of the section of stiffener was the intersection at the plate.

We calculated the eigen-values and stress distribution during vibration of the bulkhead of an actual tanker, and we obtained the following results:

(1) The lowest eigen-values of the stiffened plate contained the web frames are affected considerably by the aspect ratio of panel. When the aspect ratio is large, both the web and ordinary frames vibrate laterally, and the lowest eigen-value is small. Decreasing the aspect ratio, the ordinary frames vibrate laterally as yet, but the web frames vibrate torsionally, and then the eigen-value becomes considerably high. The more aspect ratio decreases, the more the eigen-value becomes high, and both the web and ordinary frames vibrate torsionally.

(2) When the dimensions of the web frames are constant, on the other hand, the height of the ordinary frames increase, the effect of changing the height of the ordinary frames is hardly recognized for case 1, but as increas-

ing the height the eigen-value increases for case 2, on the contrary, it decreases for case 3.

(3) If the fatigue limit of the material of the stiffened plate is 22 kg/mm^2, the maximum transverse bending stress in the plate gets to this fatigue limit, the ratio of maximum deflection to the stiffener space B is about $1/50 \sim 1/100$ for each eigen-value. The above fatigue limit of the materials is the value of mild steel under an ideal condition, but under an actual condition, this value will decrease, provided that the shape factor of the welded part, the change in quality of materials due to welding and the influence of corrosion are considered. Thus the maximum bending stress at the intersection may get to the fatigue limit even for the relative small vibrating deflection.

(4) There are only a few percentages of errors between the exact eigen-values and the approximate values obtained on the assumption that the stiffened plate arranged with an ordinary frame between two web frames alternately is semi-infinite long and the position of the neutral axis of the section of stiffener is the intersection at the plate.

References

1) Shimizu, S., On the Dynamical Stress Distribution of Stiffened Plate during Vibration, Rep. Res. Inst. Appl. Mech., Vol. XVI, No. 54, 1968.
2) Smith, C. S., Bending, Buckling and Vibration of Orthotropic Plate-Beam Structures, Jour. Ship Research, December, 1968.
3) Shimizu, S., Analysis of the Stiffened Plate Containing Web Frame, Rep. Res. Inst. Appl. Mech., Vol. XV, No. 51, 1967.
4) Anderson, R. A., *Fundamentals of Vibrations*, Macmillan, 1967, pp. 238-241.

(Received June 14, 1971)

Appendix

A 1.* Stiffness matrix for the state of plane stress of plate

The relation between the stress and the displacement at the edges j and k:

$$\left.\begin{aligned}\{\bar{P}_p\}_{jk}&=[k_p]_{11}\{\bar{U}_p\}_{jk}+[k_p]_{12}\{\bar{U}_p\}_{ki}\\ \{\bar{P}_p\}_{kj}&=[k_p]_{21}\{\bar{U}_p\}_{jk}+[k_p]_{22}\{\bar{U}_p\}_{ki}\end{aligned}\right\} \qquad \text{(A 1.1)}$$

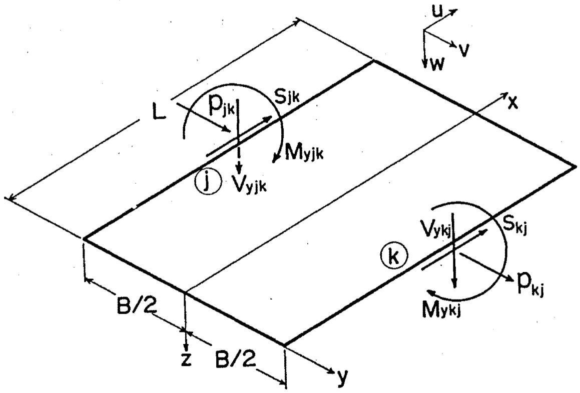

Fig. A 1.1

where

$$\{\bar{p}_p\}_{jk}=\{\bar{s}_{jk}\ \bar{p}_{jk}\},\quad \{\bar{p}_p\}_{kj}=\{\bar{s}_{kj}\ \bar{p}_{kj}\}.$$

$$\{\bar{U}_p\}_{jk}=\{\bar{u}_j\ \bar{v}_j\},\quad \{\bar{U}_p\}_{kj}=\{\bar{u}_k\ \bar{v}_k\}$$

$$[k_p]_{11}=\frac{E}{B}\begin{bmatrix}k_{11} & k_{13}\\ k_{31} & k_{33}\end{bmatrix},\quad [k_p]_{12}=\frac{B}{E}\begin{bmatrix}k_{12} & k_{14}\\ k_{32} & k_{34}\end{bmatrix}$$

$$[k_p]_{21}=\frac{E}{B}\begin{bmatrix}k_{21} & k_{23}\\ k_{41} & k_{43}\end{bmatrix},\quad [k_p]_{22}=\frac{E}{B}\begin{bmatrix}k_{22} & k_{24}\\ k_{42} & k_{44}\end{bmatrix}$$

$$k_{11}=k_{22}=\frac{1}{\Delta}\{2(ag+be)-\mu(g+e)\}$$

$$k_{12}=k_{21}=\frac{1}{\Delta}\{2(ag-be)-\mu(g-e)\}$$

$$-k_{13}=-k_{31}=k_{24}=k_{42}=\frac{1}{\Delta}\{2\mu^2-3\mu(a+b)+4ab\}$$

$$-k_{14}=-k_{41}=k_{23}=k_{32}=\frac{1}{\Delta}\mu(a-b)$$

---

* We show the formulas simply in this and following Appendices, see the references 1) and 3) on introducing the basic formulas.

$$k_{33}=k_{44}=\frac{1}{\Delta}\{2(bc+ad)-\mu(c+d)\}$$

$$k_{34}=k_{43}=\frac{1}{\Delta}\{2(bc-ad)-\mu(c-d)\}$$

$$\Delta=4\mu(\mu-2a)(\mu-2b)$$

$$a=\frac{sinh\lambda}{\lambda(sinh\lambda-\lambda)},\ b=\frac{sinh\lambda}{\lambda(sinh\lambda+\lambda)}$$

$$c=\frac{cosh\lambda-1}{\lambda(sinh\lambda-\lambda)},\ d=\frac{cosh\lambda+1}{\lambda(sinh\lambda+\lambda)}$$

$$e=\frac{cosh\lambda+1}{\lambda(sinh\lambda-\lambda)},\ g=\frac{cosh\lambda-1}{\lambda(sinh\lambda+\lambda)}$$

The stress and displacement components:

$$\left.\begin{aligned}\sigma_x&=[\phi''][k_p]\{\bar{U}_p\}sin\frac{n\pi}{L}x\\ \sigma_y&=-(\lambda/B)^2[\phi][k_p]\{\bar{U}_p\}sin\frac{n\pi}{L}x\\ \tau_{xy}&=-(\lambda/B)[\phi'][k_p]\{\bar{U}_p\}cos\frac{n\pi}{L}x\end{aligned}\right\}\qquad (A\ 1.2)$$

$$\left.\begin{aligned}u&=-(B/E\lambda)[[\phi'']+\nu(\lambda/B)^2[\phi]][k_p]\{\bar{U}_p\}cos\frac{n\pi}{L}x\\ v&=-(1/E)[(1+\nu)[\phi']+[\Delta\phi']][k_p]\{\bar{U}_p\}sin\frac{n\pi}{L}x\end{aligned}\right\}\qquad (A\ 1.3)$$

where

$$[\phi]=[f_1+f_2\quad f_1-f_2\quad f_3+f_4\quad f_3-f_4]$$

$$[\phi'']=(\lambda/B)^2[[\phi]-[\Delta\phi'']]$$

$$f_1=\frac{-(\lambda y/B)cosh(\lambda/2)sinh(\lambda y/B)+(\lambda/2)sinh(\lambda/2)cosh(\lambda y/B)}{\lambda^2(sinh\lambda+\lambda)}\cdot B^2$$

$$f_2=\frac{(\lambda y/B)sinh(\lambda/2)cosh(\lambda y/B)-(\lambda/2)cosh(\lambda/2)sinh(\lambda y/B)}{\lambda^2(sinh\lambda-\lambda)}\cdot B^2$$

$$f_3=\frac{(\lambda\cdot y/B)sinh(\lambda/2)sinh(\lambda\cdot y/B)-\{sinh(\lambda/2)+(\lambda/2)cosh(\lambda/2)\}cosh(\lambda\cdot y/B)}{\lambda^2(sinh\lambda+\lambda)}\cdot B^2$$

$$f_4=\frac{-(\lambda\cdot y/B)cosh(\lambda/2)cosh(\lambda\cdot y/B)+\{\lambda/2)sinh(\lambda/2)+cosh(\lambda/2)\}sinh(\lambda\cdot y/B)}{\lambda^2(sinh\lambda-\lambda)}\cdot B^2$$

$$[\Delta\phi'']=[\Delta f_1''+\Delta f_2''\quad \Delta f_1''-\Delta f_2''\quad \Delta f_3''+\Delta f_4''\quad \Delta f_3''-\Delta f_4'']$$

$$\Delta f_1''=\frac{2cosh(\lambda/2)cosh(\lambda\cdot y/B)}{sinh\lambda+\lambda}$$

$$\Delta f_2''=\frac{-2sinh(\lambda/2)sinh(\lambda\cdot y/B)}{sinh\lambda-\lambda}$$

$$\Delta f_3'' = \frac{-2sinh(\lambda/2)cosh(\lambda \cdot y/B)}{sinh\lambda + \lambda}$$

$$\Delta f_4'' = \frac{2cosh(\lambda/2)sinh(\lambda \cdot y/B)}{sinh\lambda - \lambda}$$

$$[k_p] = \begin{bmatrix} k_{11} & k_{12} & k_{13} & k_{14} \\ k_{21} & k_{22} & k_{23} & k_{24} \\ k_{31} & k_{32} & k_{33} & k_{34} \\ k_{41} & k_{42} & k_{43} & k_{44} \end{bmatrix}$$

A 2. Stiffness matrix for the lateral vibration of rectangular plate

The relation between the internal forces and displacement at the edges j and k:

$$\left.\begin{aligned} \{\bar{p}_b\}_{jk} &= [k'_b]_{11}\{\bar{U}_b\}_{jk} + [k'_b]_{12}\{\bar{U}_b\}_{kj} \\ \{\bar{p}_b\}_{kj} &= [k'_b]_{21}\{\bar{U}_b\}_{jk} + [k'_b]_{22}\{\bar{U}_b\}_{kj} \end{aligned}\right\} \quad \text{(A 2.1)}$$

where

$$\{\bar{P}_b\}_{jk} = \{\bar{V}_{yjk} \quad \bar{M}_{yjk}\}, \quad \{\bar{P}_b\}_{kj} = \{\bar{V}_{ykj} \quad \bar{M}_{ykj}\}$$

$$\{\bar{U}_b\}_{jk} = \{\bar{w}_j \quad \bar{\theta}_j\}, \quad \{\bar{U}_b\}_{kj} = \{\bar{w}_k \quad \bar{\theta}_k\}$$

$$[k'_b]_{11} = D\begin{bmatrix} k'_{11} & k'_{13} \\ k'_{31} & k'_{33} \end{bmatrix}, \quad [k'_b]_{12} = D\begin{bmatrix} k'_{12} & k'_{14} \\ k'_{32} & k'_{34} \end{bmatrix}$$

$$[k'_b]_{21} = D\begin{bmatrix} k'_{21} & k'_{23} \\ k'_{41} & k'_{43} \end{bmatrix}, \quad [k'_b]_{22} = D\begin{bmatrix} k'_{22} & k'_{24} \\ k'_{42} & k'_{44} \end{bmatrix}$$

(1) $\lambda^2 - k^2 < 0$

$$k'_{11} = k'_{22} = -e', \quad k'_{12} = k'_{21} = h'$$

$$k'_{13} = -k'_{24} = -(c'_k - \Delta_1), \quad k'_{14} = -k'_{23} = k'_{32} = -k'_{41} = -d'$$

$$k'_{31} = -k'_{42} = c' + \Delta_2, \quad k'_{33} = k'_{44} = a', \quad k'_{34} = k'_{43} = b'$$

$$a' = \frac{\alpha^2+\beta^2}{2B^2}\left(\frac{sin\beta/2\ sinh\alpha/2}{\Delta_1} + \frac{cos\beta/2\ cosh\alpha/2}{\Delta_2}\right)$$

$$b' = \frac{\alpha^2+\beta^2}{2B^2}\left(\frac{sin\beta/2\ sinh\alpha/2}{\Delta_1} - \frac{cos\beta/2\ cosh\alpha/2}{\Delta_2}\right)$$

$$c' = \frac{\alpha\beta}{2B^2}\left(\frac{\Delta_2}{\Delta_1} - \frac{\Delta_1}{\Delta_2}\right), \quad d' = \frac{\alpha\beta}{2B^2}\left(\frac{\Delta_2}{\Delta_1} + \frac{\Delta_1}{\Delta_2}\right)$$

$$e' = \frac{\alpha\beta(\alpha^2+\beta^2)}{2B^4}\left(\frac{cos\beta/2\ cosh\alpha/2}{\Delta_1} - \frac{sin\beta/2\ sinh\alpha/2}{\Delta_2}\right)$$

$$h'=\frac{\alpha\beta(\alpha^2+\beta^2)}{2B^4}\left(\frac{\cos\beta/2\cosh\alpha/2}{\Delta_1}+\frac{\sin\beta/2\sinh\alpha/2}{\Delta_2}\right)$$

$$c'_\kappa=c'+\frac{\alpha^2-\beta^2}{B^2},\quad A_1=(2-\nu)\frac{\lambda^2}{B^2},\quad A_2=\nu\frac{\lambda^2}{B^2}$$

$$\Delta_1=2\left(\frac{\beta}{B}\cosh\frac{\alpha}{2}\sin\frac{\beta}{2}+\frac{\alpha}{B}\sinh\frac{\alpha}{2}\cos\frac{\beta}{2}\right)$$

$$\Delta_2=2\left(\frac{\alpha}{B}\cosh\frac{\alpha}{2}\sin\frac{\beta}{2}-\frac{\beta}{B}\sinh\frac{\alpha}{2}\cos\frac{\beta}{2}\right)$$

(2) $\lambda^2-\kappa^2>0$

$$k'_{11}=k'_{22}=-e',\quad k'_{12}=k'_{21}=h',\quad k_{13}'=-k'_{24}=-k'_{31}=k'_{42}=-c'$$

$$k'_{14}=-k'_{23}=k'_{32}=-k'_{41}=d',\quad k'_{33}=k'_{44}=a',\quad k'_{34}=k'_{43}=b'$$

$$a'=\frac{\alpha^2-\beta^2}{2B^2}\left(\frac{\sinh\alpha/2\sinh\beta/2}{\Delta_2}-\frac{\cosh\alpha/2\cosh\beta/2}{\Delta_1}\right)$$

$$b'=\frac{\alpha^2-\beta^2}{2B^2}\left(\frac{\sinh\alpha/2\sinh\beta/2}{\Delta_2}+\frac{\cosh\alpha/2\cosh\beta/2}{\Delta_1}\right)$$

$$c'=\frac{\alpha\beta}{2B^2}\left(\frac{\Delta_1}{\Delta_2}+\frac{\Delta_2}{\Delta_1}\right),\quad \alpha'=\frac{\alpha\beta}{2B^2}\left(\frac{\Delta_1}{\Delta_2}-\frac{\Delta_2}{\Delta_1}\right)$$

$$e'=\frac{\alpha\beta(\alpha^2-\beta^2)}{2B^4}\left(\frac{\cosh\alpha/2\cosh\beta/2}{\Delta_2}+\frac{\sinh\alpha/2\sinh\beta/2}{\Delta_1}\right)$$

$$h'=\frac{\alpha\beta(\alpha^2-\beta^2)}{2B^4}\left(\frac{\cosh\alpha/2\cosh\beta/2}{\Delta_2}-\frac{\sinh\alpha/2\sinh\beta/2}{\Delta_1}\right)$$

$$\Delta_1=2\left(\frac{\alpha}{B}\sinh\frac{\alpha}{2}\cosh\frac{\beta}{2}-\frac{\beta}{B}\cosh\frac{\alpha}{2}\sinh\frac{\beta}{2}\right)$$

$$\Delta_2=2\left(\frac{\alpha}{B}\cosh\frac{\alpha}{2}\sinh\frac{\beta}{2}-\frac{\beta}{B}\sinh\frac{\alpha}{2}\cosh\frac{\beta}{2}\right)$$

The expressions for the bending moment and deflection:

$$\bar{M}_y=-D[[f_b'']-\nu(\lambda/B)^2[f_b]]\{\bar{U}_b\} \tag{A 2.2}$$

$$w=[f_b]\{\bar{U}_b\} \tag{A 2.3}$$

where

$$[f_b]=[f_{b1}+f_{b2}\quad f_{b1}-f_{b2}\quad f_{b3}+f_{b4}\quad f_{b3}-f_{b4}]$$

$$\{\bar{U}_b\}=\{\bar{w}_j\quad \bar{w}_k\quad \bar{\theta}_j\quad \bar{\theta}_k\}$$

(1) $\lambda^2-\kappa^2<0$

$$f_{b1}=\frac{1}{\Delta_1}\left(\frac{\beta}{B}\sin\frac{\beta}{2}\cosh\frac{\alpha y}{B}+\frac{\alpha}{B}\sinh\frac{\alpha}{2}\cos\frac{\beta y}{B}\right)$$

$$f_{b2}=\frac{1}{\Delta_2}\left(\frac{\beta}{B}\cos\frac{\beta}{2}\sinh\frac{\alpha y}{B}-\frac{\alpha}{B}\cosh\frac{\alpha}{2}\sin\frac{\beta y}{B}\right)$$

$$f_{b3}=\frac{1}{\Delta_2}\left(\sin\frac{\beta}{2}\sinh\frac{\alpha y}{B}-\sinh\frac{\alpha}{2}\sin\frac{\beta y}{B}\right)$$

$$f_{b4}=\frac{1}{\Delta_1}\left(-\cos\frac{\beta}{2}\cosh\frac{\alpha y}{B}+\cosh\frac{\alpha}{2}\cos\frac{\beta y}{B}\right)$$

(2) $\lambda^2-\kappa^2>0$

$$f_{b1}=\frac{1}{\Delta_1}\left(-\frac{\beta}{B}\sinh\frac{\beta}{2}\cosh\frac{\alpha y}{B}+\frac{\alpha}{B}\sinh\frac{\alpha}{2}\cosh\frac{\beta y}{B}\right)$$

$$f_{b2}=\frac{1}{\Delta_2}\left(\frac{\beta}{B}\cosh\frac{\beta}{2}\sinh\frac{\alpha y}{B}-\frac{\alpha}{B}\cosh\frac{\alpha}{2}\sinh\frac{\beta y}{B}\right)$$

$$f_{b3}=\frac{1}{\Delta_2}\left(-\sinh\frac{\beta}{2}\sinh\frac{\alpha y}{B}-\sinh\frac{\alpha}{2}\sinh\frac{\beta y}{B}\right)$$

$$f_{b4}=\frac{1}{\Delta_1}\left(-\cosh\frac{\beta}{2}\cosh\frac{\alpha y}{B}+\cosh\frac{\alpha}{2}\cosh\frac{\beta y}{B}\right)$$

A 3. Stiffness matrix of the beam subiected to bending moments, torsion and shearing forces

The relation between the internal forces and displacement at the intersection of the plate and stiffener:

$$\{\bar{Q}_s\}=[k_s]\{\bar{U}_A\} \tag{A 3.1}$$

where

$$\{\bar{Q}_s\}=\{\bar{q}_{Ax}\quad \bar{q}_{Ay}\quad \bar{q}_{Az}\quad \bar{w}_{Ax}\}$$

$$\{\bar{U}_A\}=\{\bar{u}_A\quad \bar{v}_A\quad \bar{w}_A\quad \bar{\theta}_A\}$$

$$[k_s]=[B]+[D]$$

$$[B]=\begin{bmatrix} B_{xx}(\lambda/B)^2 & B_{xy}(\lambda/B)^3 & B_{xz}(\lambda/B)^3 & B_{x\theta}(\lambda/B)^3 \\ B_{yx}(\lambda/B)^3 & B_{yy}(\lambda/B)^4 & B_{yz}(\lambda/B)^4 & B_{y\theta}(\lambda/B)^4 \\ B_{zx}(\lambda/B)^3 & B_{zy}(\lambda/B)^4 & B_{zz}(\lambda/B)^4 & B_{z\theta}(\lambda/B)^4 \\ B_{\theta x}(\lambda/B)^3 & B_{\theta y}(\lambda/B)^4 & B_{\theta z}(\lambda/B)^4 & B_{\theta\theta}(\lambda/B)^4+C(\lambda/B)^2 \end{bmatrix}$$

$$[D]=\begin{bmatrix} 0 & 0 & 0 & 0 \\ 0 & -(D/B^3)K_M\kappa^4 & 0 & -(D/B)K_{Gz}\kappa^4 \\ 0 & 0 & -(D/B^3)K_M\kappa^4 & (D/B)K_{Gy}\kappa^4 \\ 0 & -(D/B^2)K_{Gz}\kappa^4 & (D/B^2)K_{Gy}\kappa^4 & -(D/B)K_R\kappa^4 \end{bmatrix}$$

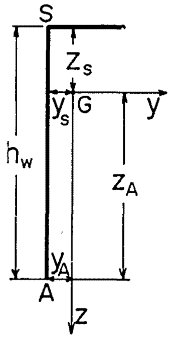

Fig. A 3.1

$$B_{xx}=EA_s$$

$$B_{xy}=B_{yx}=EA_sy_A$$

$$B_{xz}=B_{zx}=EA_sz_A$$

$$B_{x\theta}=B_{\theta x}=EA_s\{(z_A-z_s)y_A-(y_A-y_s)z_A\}$$

$$B_{yy}=E(I_z+A_sy_A{}^2)$$

$$B_{yz}=B_{zy}=E(I_{yz}+A_sy_Az_A)$$

$$B_{y\theta}=B_{\theta y}=E\{(z_A-z_s)(I_z+A_sy_A{}^2)-(y_A-y_s)(I_y+A_sy_Az_A)\}$$

$$B_{zz}=E(I_y+A_sz_A{}^2)$$

$$B_{z\theta}=B_{\theta z}=E\{(z_A-z_s)(I_{yz}+A_sy_Az_A)-(y_A-y_s)(I_y+A_sz_A{}^2)\}$$

$$B_{\theta\theta}=C_1+E\{(z-z_s)^2(I_z+A_sy_A{}^2)+(y_A-y_s)^2(I_y+A_sz_A{}^2)$$
$$-2(z_A-z_s)(y_A-y_s)(I_{yz}+A_sz_Az_s)\}$$

$$K_M=m_s/m_p,\quad K_{Gz}=m_sz_A/m_pB$$

$$K_{Gy}=m_sy_A/m_pB,\quad K_R=\Theta_A/m_pB^2$$

A 4. The dynamical equilibrium quations at the mth intersection of plate and stiffener

The equilibrium equation at the mth intersection:

$$\{\bar{P}\}_{m,m-1}+\{\bar{P}\}_{m,m+1}+\{\bar{Q}_s\}_m=0 \qquad \text{(A 4.1)}$$

where

$$\{\bar{P}\}=\{\bar{P}_p \quad \bar{P}_b\}$$

By substituting Eqs. (A 1.1), (A 2.1) and (A 3.1) into Eq. (A 4.1), we obtain the following expression,

$$\begin{bmatrix}[k_p]_{21} & \boldsymbol{0} \\ \boldsymbol{0} & [k_b]_{21}\end{bmatrix}\begin{bmatrix}\bar{U}_p \\ \bar{U}_b\end{bmatrix}_{m,m-1}+\left[\begin{bmatrix}[k_p]_{22}+[k_p]_{11} & \boldsymbol{0} \\ \boldsymbol{0} & [k_b]_{22}+[k_b]_{11}\end{bmatrix}+\begin{bmatrix} & \\ & k_s \\ & \end{bmatrix}\right]\begin{bmatrix}\bar{U}_p \\ \bar{U}_b\end{bmatrix}_m$$

$$+\begin{bmatrix}[k_p]_{12} & \boldsymbol{0} \\ \boldsymbol{0} & [k_b]_{12}\end{bmatrix}\begin{bmatrix}\bar{U}_p \\ \bar{U}_b\end{bmatrix}_{m,m+1}=\begin{bmatrix}\boldsymbol{0} \\ \boldsymbol{0}\end{bmatrix}. \qquad \text{(A 4.2)}$$

We rewrite simply as follows,

$$\boldsymbol{K}_1\boldsymbol{U}_{m,m-1}+\boldsymbol{K}_D\boldsymbol{U}_m+\boldsymbol{K}_2\boldsymbol{U}_{m,m+1}=\boldsymbol{0} \qquad \text{(A 4.3)}$$

where

$$\boldsymbol{K}_1=\begin{bmatrix}k_{21} & k_{23} & 0 & 0 \\ k_{41} & k_{43} & 0 & 0 \\ 0 & 0 & k'_{21} & k'_{23} \\ 0 & 0 & k'_{41} & k'_{43}\end{bmatrix}\begin{bmatrix}E/B \\ E/B \\ D \\ D\end{bmatrix}$$

$$\boldsymbol{K}_2=\begin{bmatrix}k_{12} & k_{14} & 0 & 0 \\ k_{32} & k_{34} & 0 & 0 \\ 0 & 0 & k'_{12} & k'_{14} \\ 0 & 0 & k'_{32} & k'_{34}\end{bmatrix}\begin{bmatrix}E/B \\ E/B \\ D \\ D\end{bmatrix}$$

$$\boldsymbol{K}_D=\begin{bmatrix}(2k_{22}E/B+B_{11}/t_p) & B_{12}/t_p & B_{13}/t_p & B_{14}/t_p \\ B_{21}/t_p & (2k_{44}E/B+B_{22}/t_p+D_{22}/t_p) & B_{23}/t_p & (B_{24}+D_{24})/t_p \\ B_{31} & B_{32} & (2k'_{22}D+B_{33}+D_{33}) & (B_{34}+D_{34}) \\ B_{41} & (B_{42}+D_{42}) & (B_{43}+D_{43}) & (2k'_{44}D+B_{44}+D_{44})\end{bmatrix}$$

$\boldsymbol{U}_m=\{\bar{u} \quad \bar{v} \quad \bar{w} \quad \bar{\theta}\}_m.$